

Laser Guidestar Satellite for Ground-based Adaptive Optics Imaging of Geosynchronous Satellites

Weston A. Marlow and Ashley K. Carlton and Hyosang Yoon and

James R. Clark and Christian A. Haughwout and Kerri L. Cahoy
Massachusetts Institute of Technology, Cambridge, MA, 02139

Jared R. Males and Laird M. Close and Katie M. Morzinski
University of Arizona, Tucson, AZ, 85721

In this study, we assess the utility of using a maneuverable nanosatellite laser guidestar from a geostationary equatorial orbit to enable ground-based, adaptive optics imaging of geosynchronous satellites with next-generation extremely large telescopes. The concept for a satellite guide star was first discussed in the literature by Greenaway in the early 1990s, and expanded upon by Albert in 2012. With a satellite-based laser as an adaptive optics guidestar, the source laser does not need to scatter, and is well above atmospheric turbulence. When viewed from the ground through a turbulent atmosphere, the angular size of the satellite guidestar is much smaller than a back-scattered source. Advances in small satellite technology and capability allow us to revisit the concept on a 6U CubeSat, measuring 10 cm by 20 cm by 30 cm. We show that a system that uses a satellite-based laser transmitter can be relatively low power (~ 1 W transmit power), operated intermittently, and requires little propellant to relocate within the geosynchronous belt. We present results of a design study on the feasibility of a small satellite guidestar and highlight the potential benefits to the space situational awareness community.

I. INTRODUCTION

A. The Need for Ground-Based Adaptive Optics

Imaging of space-based assets and astronomical objects from large, ground-based observatories is inherently limited by atmospheric turbulence. The turbulent motion of the air between a telescope and space causes index of refraction variations, which corrupt the incoming wavefront. This causes the image of a point source to blur, an effect referred to as “seeing”. Seeing is usually quantified in terms of the full-width at half maximum (FWHM) of the resultant image of a star. Typical values at astronomical observatories range from 0.5” to 1.0” in visible wavelengths [1, 2]. Importantly, this is true independent of telescope size. For an optimally performing telescope (*i.e.* diffraction-limited, as discussed in Section III A and described in Equation 1), we can compare seeing to the FWHM

of the point spread function (PSF) if a telescope were diffraction-limited and find that seeing is many times worse than diffraction limited performance. In this case FWHM is approximately λ/D where D is the diameter of the telescope and λ is the wavelength, neglecting details associated with pupil geometry. For the current generation of 6 m to 10 m telescopes, the seeing-limited FWHM is 30-90 times larger than the limit set by diffraction. This difference in FWHM means that, without compensation, there will be a dramatic loss in angular resolution. This gap will be even larger on the next generation of 24 m to 40 m ELTs, where the diffraction-limited FWHM is further reduced (improved).

In addition to degrading angular resolution, imaging through turbulence results in a loss of sensitivity. The larger PSF size increases the amount of background noise present in a measurement. When combined with the increased collecting area, the point-source sensitivity of a diffraction-limited telescope is proportional to D^4 , as opposed to D^2 in the seeing limit[3].

The atmosphere can be avoided entirely by putting telescopes in space, as in the case of the 2.4 m diameter Hubble Space Telescope (HST) and the planned 6.5 m James Webb Space Telescope (JWST) [4]. However, launch vehicle payload mass capacity and fairing sizes can limit the maximum aperture size and require more complex deployable structures, as for JWST. Building a larger telescope on the ground may be more cost effective. Ground-based telescopes have already reached 10 m in diameter (*i.e.* the Keck I and II telescopes). Construction has begun on the ELTs, with diameters ranging from 24.5 m to 39 m [5–7], and concepts exist for telescopes approaching 100 m in diameter [8]. Given the relationships for angular resolution and background limited point source sensitivity, achieving the diffraction limit on such large telescopes is highly desirable and solutions have been developed and implemented for countering the effects of atmospheric turbulence using adaptive optics (AO).

Adaptive optics allows us to recover the diffraction-limited performance of large telescopes on the ground by measuring the degradation of the incoming wavefront and correcting the wavefront in real time [3, 9, 10]. After decades of development, AO is now in routine operation at all major large-diameter astronomical observatories [11–18].

Though AO correction is now widely employed in the astronomical community, it is currently an imperfect solution for imaging GEO objects. A key drawback is that imaging with AO requires a bright reference star, or guide star, close to the object being studied. In the case of imaging GEO targets, the situation is further complicated by the sidereal motion of GEO objects relative to naturally occurring guide stars (NGS). One solution to this problem uses lasers projected from the ground up onto the sodium layer the atmosphere (at altitudes of 80 km to 100 km) to produce an artificial reference source where needed [19–24]. These laser guide stars (LGS) have significantly improved the “sky coverage” for AO for astronomical imaging, but in turn have drawbacks. A reference source within the atmosphere can be used to sample only a part of the turbulence. In addition, the source itself is an imperfect reference due to having a finite angular size (*i.e.*, it isn’t

a point source), and the brightness of the source is limited. Further improvements to the LGS solution are needed to achieve optimal performance on the new ELTs, and this paper addresses these needs by using nanosatellites with on-board lasers pointed at earth as reference sources that can be placed in desired orbits.

II. MOTIVATION

We begin motivating the use of nanosatellite guide stars by looking at the benefits of augmenting current GEO monitoring strategies with ground-based AO systems. We then describe applications for high-resolution high-Strehl imaging, highlight the fundamental limits of NGS AO performance, and briefly review some of the strategies developed to mitigate these limits.

A. Adaptive Optics for GEO Object Imaging

As the GEO belt becomes increasingly populated and contested, the need for imaging of critical commercial and military systems within the belt has continued to grow [25]. In the following sections, we present the motivation for imaging the GEO belt from earth using AO and a SGS rather than imaging using satellite-based telescopes and cameras.

1. Ground-based Imaging

Operators began using the GEO belt for Earth observation and communication beginning in the 1960s, and the belt has continued to be populated. The possibilities of collisions within the GEO belt are becoming non-negligible with the proliferation of active systems and subsequent inactive satellites, rocket bodies, and debris [26] as seen in Figure 1. Commercial and government agencies rely heavily on the continued performance of active systems within the GEO belt, and it would be useful to have the ability to image active systems for health status, confirm deployments, and to watch for proximity dangers (either orbital debris or small, active threats) [25].

The GEO and near-GEO satellite population, shown in Figure 2, gives insight into the number of active and retired systems in GEO, GEO super-synchronous and GEO sub-synchronous orbits. Likely active GEO satellites lie within the green outlined area. Objects at or above 15° inclination are not considered for these analyses, as they may be inactive systems inclined under the influence of gravitational disturbances with no station-keeping [28]. As of a 2016 full space catalog query[29], there are more than 1100 objects for which two-line element (TLE) sets have been generated with semi-major axes within the 35,000 km to 37,000 km altitude range (GEO altitude is approximately 35,786 km). Threats to the active systems in their critical orbits can come from both active and inactive satellites. Active satellites could be those possibly launched for in-GEO operations for a variety of purposes like imaging, proximity operations, or purposeful conjunctions. This paper does not contain in-depth analysis of these mission possibilities, but rather proposes methods for greater space situational awareness and space domain awareness. Decommissioned or drifting satellites

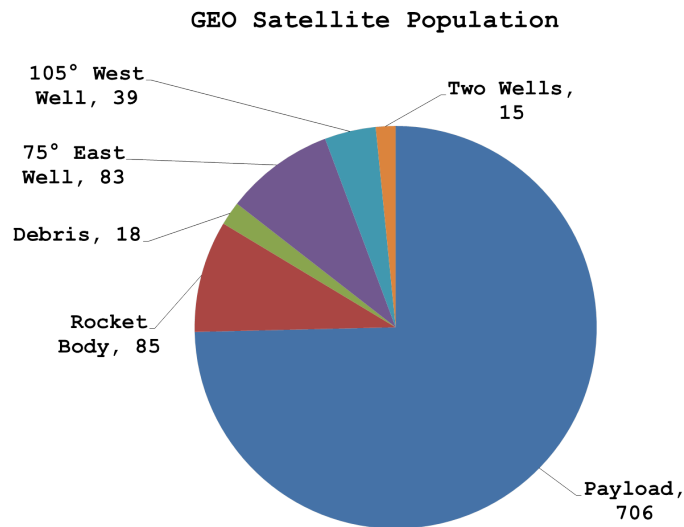


Fig. 1 Breakdown of GEO belt satellite population from analysis of satellites in libration points [27].

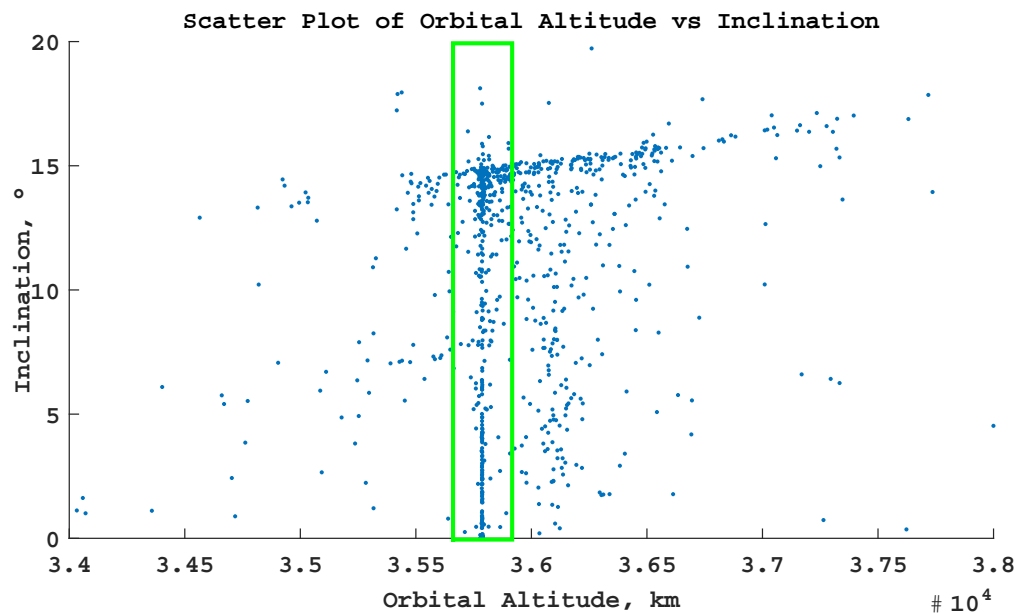


Fig. 2 Scatter plot of GEO belt objects: sub-synchronous and super-synchronous GEO orbits.

entering and exiting the GEO belt also pose a very real threat. They are naturally accelerated out of their sidereal orbits to the various libration points within the GEO belt and to greater inclinations [28]. Ground-based radar tracking and TLE analysis can give satellite operators warning of possible conjunction events, but real-time imaging of active, high-value assets (HVAs) would give direct observation of near-conjunction events or possible proximity operations of smaller GEO-located satellites.

B. Optical Performance for Imaging GEO Objects

The importance of high-quality imaging of GEO HVAs for spacecraft health and SSA, in addition to the potential use as a photometric calibration target [30], are compelling reasons to revisit the SGS concept as presented here. While we do not delve into analysis and simulation of the imagery possible with ground-based assets, previous work from the University of Hawaii and the University of Arizona has been done to examine the utility and feasibility of imaging the GEO belt with ground systems [31]. We present a key figure from their findings in Figure 3 which shows results from an analysis which studied the Advanced Electro Optical System (AEOS) telescope at Haleakala Observatory in Hawaii. These simulated results are for the 3.67 m system that uses AO to perform image correction and show a simulated scene resolving a main target (5 m x 50 m class) communications satellite clearly distinguished from the surrounding microsatellites. The results appear promising, given the relatively modest telescope size as compared to the next generation ELTs, along with an exposure time of three seconds (we show the possibility of much longer integration times in Section IV B and in Figure 8). The results show the target HVA and nearby microsatellites or orbital debris are clearly distinguishable.

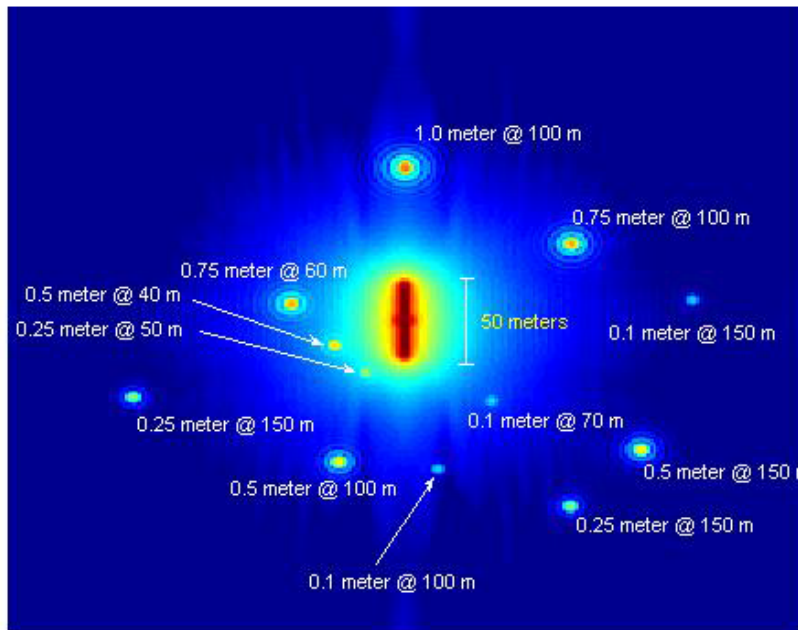


Fig. 3 AO simulated results of the AEOS telescope with a 3-second integration time [31].

Equally convincing results from the University of Cambridge using ground-based interferometric systems are presented in Figure 4 using synthetic aperture interferometric imaging [25]. The panels show a truth satellite image at $1.65 \mu\text{m}$ of magnitude 8 (left), a reconstructed interferometric image

(middle) using capabilities of the Magdalena Ridge Observatory Interferometer, and adding data from an 8 m-class telescope non-redundantly masked to increase image fidelity (right). The authors propose using existing telescope systems with non-redundantly masked apertures combined with AO on large diameter telescopes (8 m for their analysis and simulation). This approach would allow the SSA community to gather high quality images of the brightest GEO objects using larger, single telescopes to achieve the shorter baselines needed for such an approach. The results presented here show that the target satellite can be seen in detail down to 1.4 m resolution at GEO altitudes. This paper focuses on the feasibility and utility of a SGS system and its application to AO, and does not further investigate the use of interferometric imaging, but both advanced electro-optical imaging and interferometry would benefit from the use of a SGS as a predictable, bright calibration source or artificial guide star.

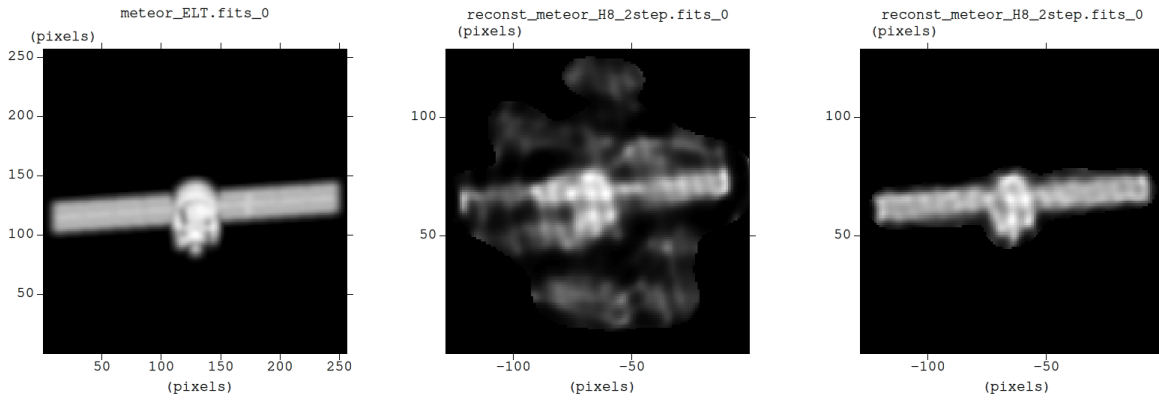


Fig. 4 Interferometric imaging simulation results [25].

1. On-orbit Imaging

Direct on-orbit imaging presents challenges for monitoring and diagnosing assets within the GEO belt. Given the volume and size constraints of nanosatellites, as we discuss in this paper, the required aperture for imaging at the visible band ($\lambda = 550$ nm) quickly reaches sizes that present a challenge for these small form-factor buses.

The angular resolution is dictated by the diffraction-limited relationship (known as the *Rayleigh limit*) between λ and the aperture size D , and is given by:

$$\theta \approx 1.22 \frac{\lambda}{D} \quad (1)$$

Further detail about diffraction-limited seeing is presented in Section III A. Since we are considering how well a space-based telescope could do at high resolution imaging of GEO objects, we can use the diffraction-limited relationship, since the imager will not be affected by atmospheric disturbances. We have chosen a feature resolution of 10 cm to help enable the resolution set as a

goal by the 2015 Defense Advanced Research projects Agency (DARPA) Request for Information on technology solutions for space domain awareness [32]. The distance to a target, d , is needed for determining aperture size. Analyzing catalog data for satellites that have semi-major axes within a ± 6 km altitude range of GEO altitude, we find a mean orbital distance between 480 (assumed) actively controlled systems within the GEO belt to be $d \approx 550$ km. This active population size agrees closely with analysis done at MIT Lincoln Laboratory in 2005 [28] and will serve as our assumption for the GEO population for the purposes of determining orbiting imager system parameters. With this d we can determine the angular diameter of a 10 cm resolved feature of 0.18μ rad. The required aperture diameter for such an on-orbit diffraction-limited GEO-based system would be $D = 3.7$ m (for $\lambda = 550$ nm). A system this size is roughly 150% larger than the HST. Such a system would require a significant investment given current launch vehicle and fairing sizes, as well as propellant for stationkeeping and maneuvering.

Alternatively, a system might be designed to fit on a 6U CubeSat ($10 \text{ cm} \times 20 \text{ cm} \times 30 \text{ cm}$) that can image to 10 cm feature resolution in space. If we assume that the imaging aperture on such a system is constrained by the smallest dimension of the CubeSat bus, this gives us an aperture of about 10 cm in diameter. Using Equation 1 we can determine the distance needed to achieve 10 cm linear resolution on GEO targets in the visible band ($\lambda = 550$ nm). Assuming diffraction-limited optics, we find that a CubeSat would need to be within approximately 15 km of the GEO belt altitude. The available volume in such a system would likely be dominated by the optical payload, and would limit the remaining volume to fit a propulsion system. This leaves the satellite as a largely-drifting system, meaning that imaging opportunities would come infrequently, only as often as the satellite passes "below" or "above" the target of interest via circular supersynchronous or subsynchronous orbits. The topic of in-space imaging with CubeSats, however, warrants more detailed discussion and consideration of new technology developments in advanced optics and deployables for CubeSats that is currently beyond the scope of this paper.

We propose an alternative method for observation using ground-based imaging of GEO targets with the use of the large, next-generation astronomical AO telescopes that use SGS systems for their reference sources. These proposed approaches could augment or minimize the need for dedicated space-based GEO-imaging satellites. We also present the types of ground stations required for reasonable resolutions, and the results of preliminary orbital analyses.

2. *Satellite Guide Stars*

The concept for a satellite guide star (SGS) was originally proposed by Greenaway [33, 34], in addition to proposals to use satellite laser sources as photometric calibration targets [30], and a satellite-based approach has many potential benefits over a LGS system, especially if the cost of the satellite and access to space is reduced. The laser does not need to scatter (either Rayleigh

backscatter or scatter from the high altitude sodium layer as in LGS systems) with returned power high enough to generate a detectable reference source. A system that uses a satellite-based laser projected downwards with a narrow beamwidth can use a low-power laser, even if it is at a larger distance. A SGS will also be well above all atmospheric turbulence, and will provide a small angular size reference source. A satellite-based laser guidestar can overcome the cone effect, the need for a tip/tilt guide star and provide a very high photon flux to the WFS. This was the motivation for the PHAROS concept [33, 34]. Until recently, launching a system like this into space was as complex, if not more so than ground based LGS systems, and launch costs were prohibitive.

However, in recent years there has been a paradigm shift to smaller, less expensive satellites [35]. Miniature, common form factor satellites, called CubeSats, have emerged over the past decade, enabling quick access to space at a fraction of the cost. The small $10\text{ cm} \times 10\text{ cm} \times 10\text{ cm}$ cube (1U CubeSat) offers a common bus size that allows for easy integration as an auxiliary payload on traditional satellite launches via the standard Poly-Picosatellite Orbital Deployer (P-POD), and the more recent Canisterized Satellite Dispenser[36] (CSD) or others. This has enabled rapid technology testing on-orbit and mission concept development. The standardization of small ride-share spacecraft has spurred the miniaturization of the needed subsystem electronics, optics, attitude control, communication, power, propulsion, etc., which are now available commercially “off the shelf” (COTS) for CubeSats. This revolution in small satellite technology motivates us to revisit the SGS system on a small satellite platform, such as a 6U CubeSat, measuring $10\text{ cm} \times 20\text{ cm} \times 30\text{ cm}$ and typically with mass of $\leq 14\text{ kg}$.

III. DESIGN STUDY ASSUMPTIONS

In the following sections we discuss the design for the proposed CubeSat platform. While our design would work for a number of different wavelengths for the laser, and in fact could support multiple different lasers, we initially use 850 nm and provide rationale for that selection. For light pollution reasons, it is very important to emphasize that the laser would normally be off, and only commanded on when ground-based observations were desired, and when on, has an extremely narrow beamwidth.

A. Resolution

We can infer the ability of the ELTs with AO to image GEO objects by considering their ability to resolve features or objects at GEO altitudes. Using Equation 1, we obtain the following upper limits for angular resolution and corresponding linear resolution metrics at GEO altitudes for the different ELTs, assuming their performance is meeting the Rayleigh criterion. We consider the Giant Magellan Telescope (GMT), the Thirty Meter Telescope (TMT), the European Extremely Large Telescope (EELT), and the Overwhelmingly Large Telescope (OWL).

Table 1 Rayleigh limit resolution for ELTs using $\lambda=550$ nm.

Telescope	Diameter	Angular Resolution	Lin. Res. at GEO	Location	Ref.
GMT	24.5 m	0.0056"	98 cm	Las Campanas Observatory, Chile	[5]
TMT	30 m	0.0046"	80 cm	Mauna Kea, Hawaii	[6]
EELT	39 m	0.0035"	62 cm	Cerro Armazones, Chile	[7]
OWL	100 m	0.0014"	24 cm	<i>concept only</i>	[8]

B. Choice of Wavelength and Brightness Goal

It is desirable to have the SGS transmit at wavelengths that are not visible or harmful to the human eye (the maximum permissible exposure (MPE) level for a ten second exposure is about 100 mW/cm² for a 1550 nm laser [37]), and for which we can use inexpensive detectors that do not require complex system support, such as cooling. It is also beneficial if the wavelengths are selected such that the transmitter is power-efficient and can close a link from GEO with sufficient margin.

Several considerations drive our choice of wavelength for the SGS beacon. Current AO systems most often use silicon based detectors in the WFS, so designing for existing systems implies a wavelength $\lambda < 1000$ nm. In Figure 5 we show the bandpass for the Magellan AO system (MagAO) WFS [18]. MagAO is mounted on the 6.5 m Magellan Clay telescope at Las Campanas Observatory (LCO). Its WFS has a central wavelength of 780 nm, and peak sensitivity around 850 nm.

In addition to MagAO, other current generation AO systems such as the Large Binocular Telescope AO (LBT AO) (MagAO is essentially a clone [17]) and the Gemini Planet Imager (GPI) have WFS that work at about *I* band (806 nm) as well.

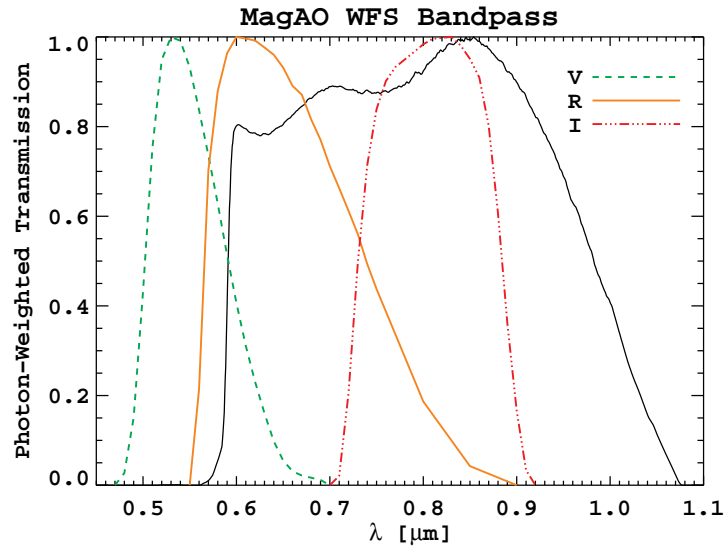


Fig. 5 The Magellan AO system WFS bandpass (solid black curve). Taken from <https://visao.as.arizona.edu/observers/>.

We use MagAO to establish the SGS minimum photon flux requirement. MagAO is noteworthy because it delivers Strehl ratios greater than 40% in the optical ($\lambda < 1000$ nm) on bright NGSs [38]. In Figure 6 we illustrate this capability, showing WFE versus NGS brightness in the WFS bandpass. The dotted lines are predictions from detailed analytic performance modeling. The asterisks are on-sky measurements at various wavelengths, and the red curve and points correspond to good ($\sim 25\%$) conditions, blue corresponds to median conditions, and black to poor ($\sim 75\%$). It is clear that a star brighter than ~ 8 mags is required for optimum performance. There is a sharp drop in performance (increasing WFE) starting at $m \sim 8$ mags.

Integrated over the spectrum of Vega in the MagAO WFS bandpass, which is centered at 0.78 microns, a zero-magnitude star has a flux of $F_{ref} = 5 \times 10^9$ photons/m²/s [39]. Therefore, to achieve an $m \sim 8$ magnitude star or brighter, using Equation 2 the minimum photon flux requirement for the system is $F = 3.15 \times 10^6$ photons/m²/s.

$$m - m_{ref} = -2.5 \log_{10} \left(\frac{F}{F_{ref}} \right) \quad (2)$$

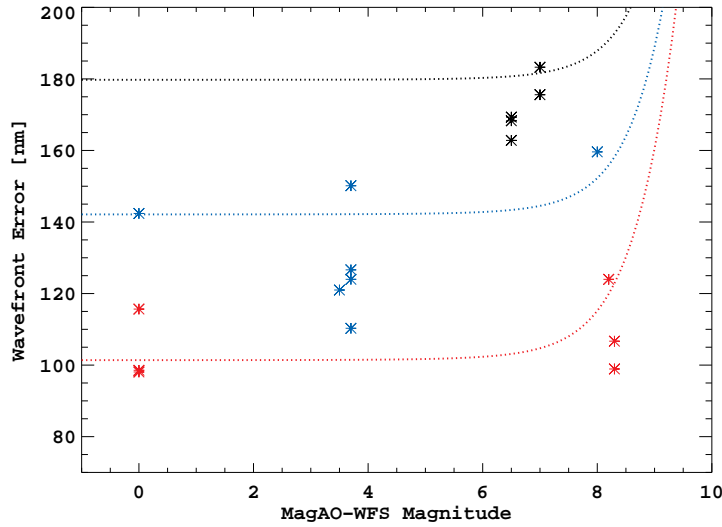


Fig. 6 MagAO performance versus guide star magnitude. On-sky points are from the MagAO VisAO camera [38].

IV. GEO OBSERVATION ANALYSIS

We next examine the use of a space-based 850 nm laser guide star system operating within the GEO belt.

A. Proposed Concepts of Operation

Three main concepts of operations are presented for AO imaging of the GEO belt for space situational awareness or asset health and status assessment: sub-synchronous SGS, super-synchronous

SGS, and a revisit mission. Sub-synchronous GEO satellites are those that have slightly lower altitudes than the GEO altitude and thus move at a faster orbital rate than GEO motion. Objects in these orbits migrate relative to the GEO belt in an eastward direction. Super-synchronous are the converse, having higher altitudes and moving relative to the belt in a westward motion. A diagram of the super-synchronous and sub-synchronous orbits relative to a standard GEO satellite are shown in Figure 7 (b), upper, lower and middle orbits, respectively.

We propose that SGS operators would be able to control the relative rate at which the satellite passes above or below a target, thus controlling the integration time for the system. For lengthy integrations, operators would be able to move into proximity of a target system and match the sidereal rate to allow for indefinite imaging. Figure 7 (a) shows the maximum in-plane distances that a GEO SGS system should maintain to fall within the same isoplanatic patch as the target satellite. The diagram presents a sub-synchronous example. Finally, a co-orbital revisiting mission is presented in Figure 7 (c). Here, the sub-synchronous guide star allows imaging during a fast, lower altitude pass but can raise altitude to allow for a secondary integration opportunity of the same target.

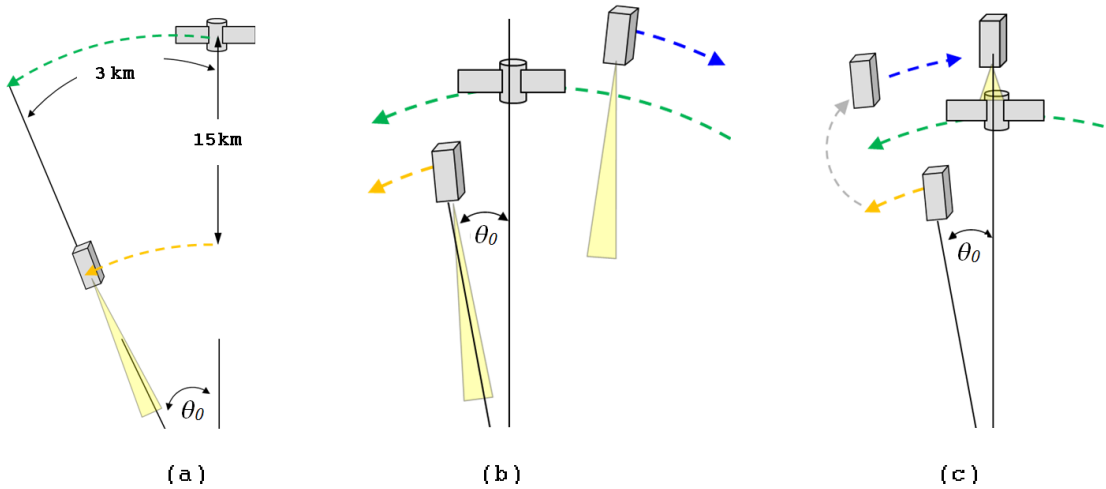


Fig. 7 GEO-based SGS (a) relative distances (b) Target with sub-synchronous and super-synchronous SGS (c) Revisiting with a change in altitude.

B. GEO SGS Delta-V Analysis

Here we discuss the mission design impact for executing the different scenarios in terms of delta-V. The costs for executing these imaging maneuvers are fairly modest as compared to those presented for astronomical targets. These costs are shown in Figure 8 for a single imaging event with variable integration times. It can be seen that as the desired integration times increase, the cost to change from a standard GEO altitude decreases. Figure 8 shows the continuum of delta-V costs for only 1.2 seconds of integration time and their associated orbital altitudes. The integration time here refers to the total available time that the SGS is within the isoplanatic patch with the

target satellite.

In considering these missions, we must also look at the requirement to maintain a safe distance from the imaging target or other GEO objects. Avoiding a SGS-caused conjunction with the satellite of interest is extremely important. Since the guide star satellite would be moving in the GEO belt relative to the target, it is critical to keep track of its position. For example, when the integration times reach greater than approximately 14 hours, the guide star satellite orbital radius falls within 500 meters of the target satellite (for both sub- and super-synchronous orbits). For lengthy integration times, a stop-and-perch approach might work best, but would require more propellant to enable. For example, this could be accomplished by approaching the target satellite and matching orbital speeds to reside in near-orbit until the imaging is complete, as seen in concept of operations in Section IV A. Once finished with imaging a target, the SGS could then be commanded to move to other longitudes of the GEO belt.

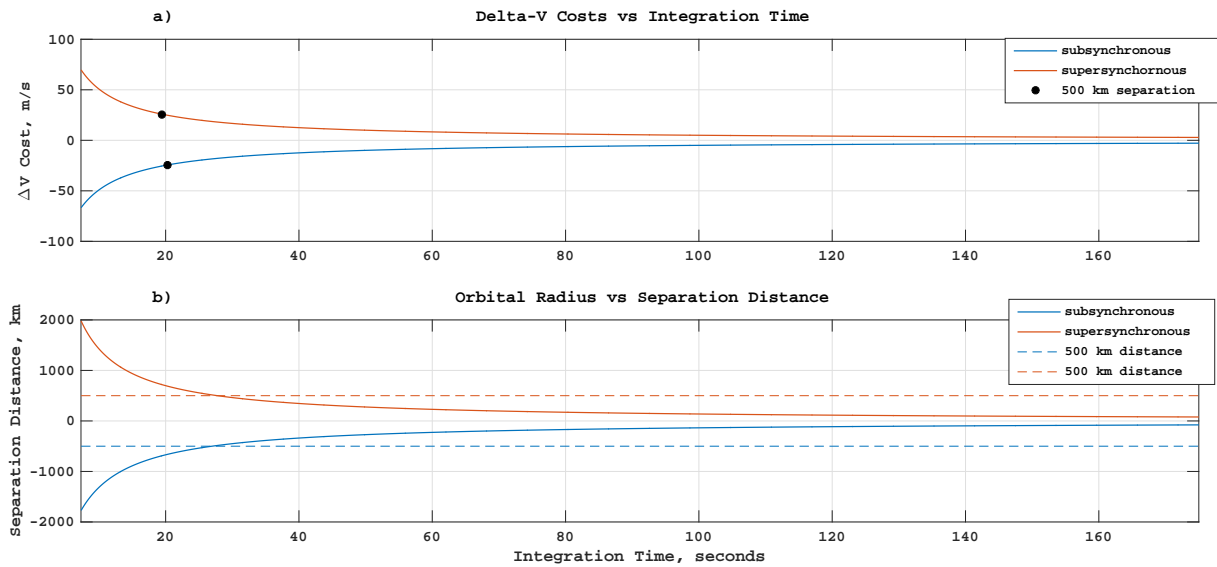


Fig. 8 a) Delta-V costs for respective integration and b) orbital radius difference between the SGS and target satellite.

A GEO-based guide star satellite with propulsion has the flexibility of re-positioning within the orbital belt. Here, only in-plane equatorial maneuvers are proposed, in an effort to keep maneuvers within the capabilities of a CubeSat. Results of the delta-V analysis are presented in Figure 9, showing the delta-V costs associated with moving the guide star satellite up to 10° in longitude eastward (sub-synchronous) or westward (super-synchronous) relative to an arbitrary geostationary point using a transfer ellipse and re-circularization into GEO. Only two-body mechanics are assumed, along with impulsive maneuvering. For missions where traversal time is not an issue, a 10° longitude change can be accomplished for less than 10 m/s in delta-V for a 30-day transfer time. Figure 9 presents the lower bound as a 24-hour transfer time. Sub-synchronous (eastward) and super-synchronous (westward) transfers are presented for the bounding cases (for this paper) of 1° and

10° longitude changes over 1 through 30 day transfer times. The ΔV costs include speed changes into transfer ellipses and re-circularization into GEO orbits.

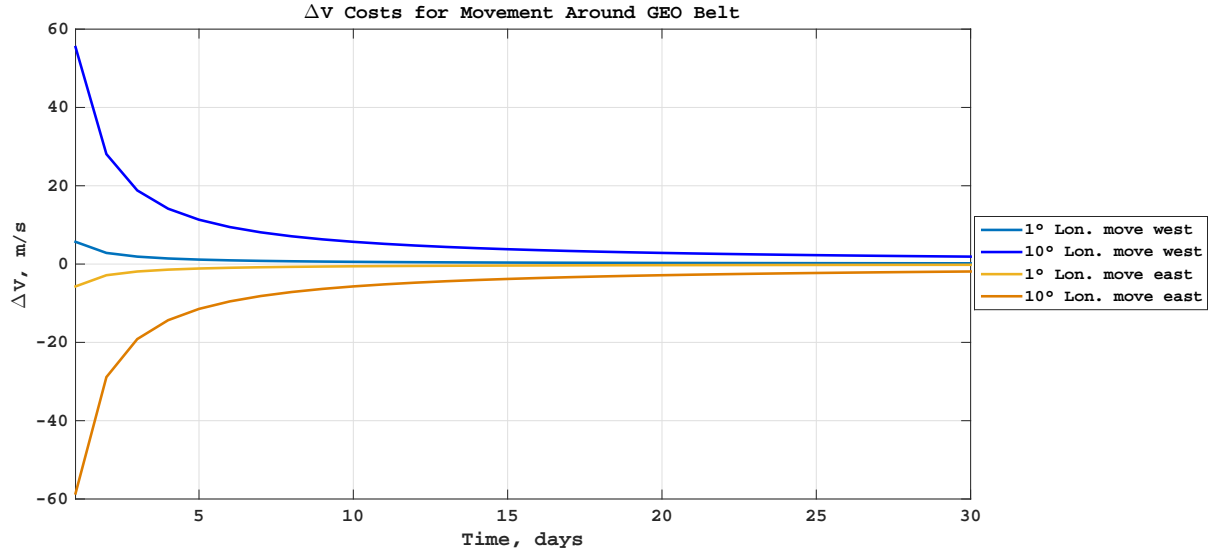


Fig. 9 Total delta-V costs associated with longitude changes within GEO.

We have shown that a GEO-based guide star satellite can be useful for potential commercial or government related tasking. These artificial guide star systems can act as re-positionable calibration sources for different ground systems with relatively small delta-V costs. They can serve for adaptive optics imaging of the GEO belt for HVA monitoring and space situational awareness assessments.

V. DISCUSSION & CONCLUSIONS

Laser payload optical components are commercially available that would satisfy the mission requirements of 10 W input electrical power (with up to at least 20 W), with about 1 W of output optical power. The current state of the art in CubeSat and small-satellite ADCS should support the required 60" (1.82 mrad) fine-pointing capability on a 6U CubeSat platform. This study shows that the SGS concept appears to be viable in the context of a CubeSat mission. Providing a bright ($< \sim 8$ mags) reference source for AO at arbitrary positions on the sky would enable diffraction limited observations with large telescopes on any target. Using only natural guide stars, such observations are limited to $< 0.01\%$ of the sky. With LGS, the need for a tip/tilt guide star limits such observations to $< \sim 10\%$ and generally requires observations at longer wavelengths for true diffraction limited imaging. In contrast, the SGS concept enables observations of essentially 100% of the sky, including objects in GEO, at the diffraction limit. With the coming 24 to 39 m ELTs, this translates to sub-meter-scale resolution on GEO objects. Used with long baseline interferometers, an SGS will help enable the 10 cm resolution at GEO set as a goal by DARPA.

There are several key technical trade studies that will be needed in preparation for an SGS mission, specifically relating to the design of the laser transmitter payload, the spacecraft's ADCS

system, and the means of propulsion. For the laser transmitter, both high-power laser diode (HPLD) and master oscillator power amplifier (MOPA) architectures are possibilities for generating the required laser light. The HPLD architecture has the advantage of being simpler, lighter, and more power efficient, while the MOPA architecture has the advantage of being very easily scaled to larger optical transmit powers. This trade is partially dependent on the required laser pulse and timing characteristics, the choice of the optical transmit wavelength to be used and whether or not any nonlinear optical elements will be implemented to achieve frequency doubling.

A comprehensive analysis of the spacecraft's navigation and ADCS system must be performed. For the initial feasibility analysis on this system, factors like pointing stability and wheel-induced jitter, orbit determination accuracy, and timing accuracy were ignored, but must be considered in future work. Although these effects may put an upper bound on the maximum achievable performance of the SGS, they are not expected and substantially affect the baseline feasibility analysis performed here.

The trade study on which propulsion system to implement must also be revisited as new technologies become available. For a sample concept of operations to image ten separate target satellites in one year, we estimate that it would take 87 m/s of delta-V, including 3.8 m/s delta-V to navigate from a GEO drop-off location that is 10° in longitude away from the first desired target in 15 days. Assuming longitude changes of 10° east or west between targets and a 20 day transfer time, this mission plan would enable approximately 150 days of potential imaging time across the ten targets. While our baseline analysis concluded that a green monopropellant system best fits this need due to its high ISP and high thrust, with further development another solution may prove superior and allow a longer mission and more sophisticated maneuvers. This trade would also require further consideration of thermal effects depending on how much heat the thruster rejects to the spacecraft. Propulsion that enables CubeSats to maneuver with significant amounts of delta-V within relatively short timescales is a key area for further technology development and demonstration.

Several remaining mission or ConOps trades exist as well. While this paper focuses on the feasibility and utility of a SGS system applied to adaptive optics, it does not cover applications of the SGS system as a photometric calibration source. In this role, the SGS system could potentially be of great value in interferometric imaging and advanced electro-optical imaging. Whether or not using the SGS in this application would place any constraints on its primary AO mission has not been considered here and would require additional analysis.

Additionally the trade between integration time, the frequency of opportunities for AO observations, and number of satellites must be considered. It is generally desirable to have longer integration times. This would be achieved by placing the spacecraft in a higher orbit with a longer orbital period, which unfortunately decreases the number of opportunities for AO observations in a manner that is proportional to the orbital period. This is due to the limitation of only having one opportunity per orbit. Due to the low cost nature of cubesats, it may be possible to deploy

a constellation of satellite guide stars which would allow multiple observations per orbital period. The operational considerations of utilizing such a constellation have not been investigated here but the concept is worthy of further investigation.

Acknowledgments

Jared R. Males was supported under contract with the California Institute of Technology (Caltech) funded by NASA through the Sagan Fellowship Program executed by the NASA Exoplanet Science Institute.

Jim Clark was supported by the MIT Deshpande Center for Technological Innovation.

Hyosang Yoon was supported by the Samsung Scholarship.

References

- [1] S. Els, M. Schöck, E. Bustos, J. Seguel, J. Vasquez, D. Walker, R. Riddle, W. Skidmore, T. Travouillon, and K. Vogiatzis, *Publications of the Astronomical Society of the Pacific* **121**, 922 (2009)
- [2] D. J. Floyd, J. Thomas-Osip, and G. Prieto, *Publications of the Astronomical Society of the Pacific* **122**, 731 (2010)
- [3] J. W. Hardy, *Adaptive optics for astronomical telescopes* (Oxford University Press on Demand, 1998)
- [4] B. D. Seery, in *Astronomical Telescopes + Instrumentation* (International Society for Optics and Photonics, 2003) pp. 170–178
- [5] R. A. Bernstein, P. J. McCarthy, K. Raybould, B. C. Bigelow, A. H. Bouchez, J. M. Filgueira, G. Jacoby, M. Johns, D. Sawyer, S. Sheckman, *et al.*, *SPIE Astronomical Telescopes + Instrumentation*, , 91451C (2014)
- [6] J. Nelson and G. H. Sanders, *SPIE Astronomical Telescopes + Instrumentation*, , 70121A (2008)
- [7] R. Tamai and J. Spyromilio, *SPIE Astronomical Telescopes+ Instrumentation*, , 91451E (2014)
- [8] P. Dierickx and R. Gilmozzi, *Astronomical Telescopes and Instrumentation*, , 290 (2000)
- [9] J. M. Beckers, *Annual Review of Astronomy and Astrophysics* **31**, 13 (1993)
- [10] R. Tyson, *Principles of Adaptive Optics, Third Edition, by Robert Tyson, pp. 314. CRC Press, Sep 2010. ISBN-10: 1439808589. ISBN-13: 9781439808580* (2010)
- [11] M. Troy, R. G. Dekany, G. L. Brack, B. R. Oppenheimer, E. E. Bloemhof, T. Trinh, F. G. Dekens, F. Shi, T. L. Hayward, and B. R. Brandl, *Astronomical Telescopes and Instrumentation*, , 31 (2000)
- [12] F. P. Wildi, G. Brusa, M. Lloyd-Hart, L. M. Close, and A. Riccardi, *Optical Science and Technology, SPIE's 48th Annual Meeting*, , 17 (2003)
- [13] G. Herriot, S. Morris, A. Anthony, D. Derdall, D. Duncan, J. Dunn, A. W. Ebberts, J. M. Fletcher, T. Hardy, B. Leckie, *et al.*, *Astronomical Telescopes and Instrumentation*, , 115 (2000)
- [14] P. Wizinowich, D. Acton, C. Shelton, P. Stomski, J. Gathright, K. Ho, W. Lupton, K. Tsubota, O. Lai, C. Max, *et al.*, *Publications of the Astronomical Society of the Pacific* **112**, 315 (2000)
- [15] G. Rousset, F. Lacombe, P. Puget, N. N. Hubin, E. Gendron, T. Fusco, R. Arsenault, J. Charton, P. Feautrier, P. Gigan, *et al.*, *Astronomical Telescopes and Instrumentation*, , 140 (2003)
- [16] Y. Minowa, Y. Hayano, S. Oya, M. Watanabe, M. Hattori, O. Guyon, S. Egner, Y. Saito, M. Ito, H. Takami, *et al.*, *SPIE Astronomical Telescopes+ Instrumentation*, , 77363N (2010)

- [17] S. Esposito, A. Riccardi, L. Fini, A. T. Puglisi, E. Pinna, M. Xompero, R. Briguglio, F. Quirós-Pacheco, P. Stefanini, J. C. Guerra, *et al.*, *SPIE Astronomical Telescopes + Instrumentation*, , 773609 (2010)
- [18] L. M. Close, J. Males, K. Morzinski, D. Kopon, K. Follette, T. Rodigas, P. Hinz, Y. Wu, A. Puglisi, S. Esposito, *et al.*, *The Astrophysical Journal* **774**, 94 (2013)
- [19] R. Foy and A. Labeyrie, *Astronomy and Astrophysics* **152**, 129 (1985)
- [20] L. A. Thompson and C. S. Gardner, *Nature* **328**, 229 (1987)
- [21] R. Q. Fugate, L. M. Wopat, D. L. Fried, G. A. Ameer, S. L. Browne, P. H. Roberts, G. A. Tyler, B. R. Boeke, and R. E. Ruane, *Nature* **353**, 144 (1991)
- [22] M. Lloyd-Hart, J. R. P. Angel, B. Jacobsen, D. Wittman, R. Dekany, D. McCarthy, E. Kibblewhite, W. Wild, B. Carter, and J. Beletic, *The Astrophysical Journal* **439**, 455 (1995)
- [23] C. E. Max, S. S. Olivier, H. W. Friedman, J. An, K. Avicola, B. V. Beeman, H. D. Bissinger, J. M. Brase, G. V. Erbert, D. T. Gavel, *et al.*, *Science* **277**, 1649 (1997)
- [24] P. L. WIZINOWICH, D. Le Mignant, A. H. Bouchez, R. D. Campbell, J. C. Chin, A. R. Contos, M. A. van Dam, S. K. Hartman, E. M. Johansson, R. E. Lafon, *et al.*, *Publications of the Astronomical Society of the Pacific* **118**, 297 (2006)
- [25] J. Young, C. Haniff, and D. Buscher, in *2013 IEEE Aerospace Conference* (2013) p. 9
- [26] R. A. Leclair and R. Sridharan, in *Space Debris*, ESA Special Publication, Vol. 473, edited by H. Sawaya-Lacoste (2001) pp. 463–470
- [27] M. A. Skinner *et al.*, in *Proceedings of the Advanced Maui Optical and Space Surveillance Technologies Conference* (2013)
- [28] R. Jehn, V. Agapov, and C. Hernández, in *4th European Conference on Space Debris*, ESA Special Publication, Vol. 587, edited by D. Danesy (2005) p. 373
- [29] Space-Track, accessed February 17, 2016, <https://www.space-track.org>
- [30] J. Albert, *The Astronomical Journal* **143** (2012)
- [31] D. Hope, S. Jefferies, and C. Giebink, in *Proceedings of the Advanced Maui Optical and Space Surveillance Technologies Conference* (2008)
- [32] *Request for Information: Technology Solutions for Passive, Sparse Aperture Imaging for Space Domain Awareness*, Special Notice DARPA-SN-15-38 (DARPA, 2015)
- [33] A. H. Greenaway, *Proc. SPIE* **1494**, 8 (1991)
- [34] A. H. Greenaway and S. E. Clark, *Proc. SPIE* **2120**, 206 (1994)
- [35] E. Hand, *Science* **348**, 172 (2015)
- [36] Planetary Systems Corporation, accessed April 21, 2015, http://www.planetarysystemscorp.com/?post_type=product&p=448
- [37] *American National Standard for Safe Use of Lasers*, Tech. Rep. ANSI Z136.1 (American National Safety Institute, 2014)
- [38] J. R. Males, L. M. Close, K. M. Morzinski, Z. Wahhaj, M. C. Liu, A. J. Skemer, D. Kopon, K. B. Follette, A. Puglisi, S. Esposito, *et al.*, *The Astrophysical Journal* **786**, 32 (2014)
- [39] R. C. Bohlin, in *The Future of Photometric, Spectrophotometric and Polarimetric Standardization*, Astronomical Society of the Pacific Conference Series, Vol. 364, edited by C. Sterken (2007) p. 315